Challenges and opportunities in nasal subunt vaccine delivery : mechanistic studies using ovalbumin as a model antigen

Slütter, B.A.

4

Nasal vaccination with N-trimethyl chitosan and PLGA based nanoparticles: Nanoparticle characteristics determine quality and strength of the antibody response in mice against the encapsulated antigen

Bram Slütter
Chantal Keijzer
Niels Hagenaars
Eric Kaijzel
Patrick Augustijns
Joke Bouwstra
Wim Jiskoot
Suzanne Bal
Roel Mallants
Ivo Que
Willem van Eden
Clemens Löwik
Femke Broere

Vaccine 2010 28(38):6282-91

Abstract

Nasal vaccination is a promising, needle-free alternative to classical vaccination. Nanoparticulate delivery systems have been reported to overcome the poor immunogenicity of nasally administered soluble antigens, but the characteristics of the ideal particle are unknown. This study correlates differences in physicochemical characteristics of nanoparticles to their adjuvant effect, using ovalbumin (OVA)-loaded poly(lactic-co-glycolic acid) nanoparticles (PLGA NP), N-trimethyl chitosan (TMC) based NP (TMC NP) and TMC-coated PLGA NP (PLGA/TMC NP).

PLGA NP and PLGA/TMC NP were prepared by emulsification/solvent extraction and TMC NP by ionic complexation. The NP were characterized physicochemically. Their toxicity and interaction with and stimulation of monocyte derived dendritic cells (DC) were tested *in vitro*. Furthermore, the residence time and the immunogenicity (serum IgG titers and secretory IgA levels in nasal washes) of the nasally applied OVA formulations were assessed in Balb/c mice.

All NP were similar in size, whereas only PLGA NP carried a negative zeta potential. The NP were non toxic to isolated nasal epithelium. Only TMC NP increased the nasal residence time of OVA compared to OVA administered in PBS and induced DC maturation. After i.m. administration all NP systems induced higher IgG titers than OVA alone, PLGA NP and TMC NP being superior to PLGA/TMC NP. Nasal immunization with the slow antigen-releasing particles, PLGA NP and PLGA/TMC NP, did not induce detectable antibody titers. In contrast, nasal immunization with the positively charged, fast antigen-releasing TMC NP led to high serum antibody titers and sIgA levels.

In conclusion, particle charge and antigen-release pattern of OVA-loaded NP has to be adapted to the intended route of administration. For nasal vaccination, TMC NP, releasing their content within several hours, being mucoadhesive and stimulating the maturation of DC, were superior to PLGA NP and PLGA/TMC NP which lacked some or all of these characteristics.

Introduction

The nasal cavity is one of the most promising administration sites for vaccines. The nose is easily accessible, low on proteolytic enzymes compared to the oral route and has interesting immunological characteristics. As the nasal cavity is a major route of entry for pathogens, the nasal epithelium is equipped with a large amount of immune cells to fight off infection and is capable of producing secretory IgA. Several studies have shown systemic as well as local antibody responses after nasal administration of an antigen [1-7]. Administration of subunit vaccines alone, however, seldom leads to a protective antibody response. The residence time of a soluble antigen in the nose is limited, which results in a very small dose reaching antigen-presenting cells (e.g. dendritic cells) in the sub epithelial region. Moreover, subunit vaccines are often poorly immunogenic as they lack the necessary danger signals to activate dendritic cells (DC) and subsequently, T-cells.

To overcome these obstacles, encapsulating antigen into particulate systems is a popular method [8]. Particles prepared with mucoadhesive substances can increase the antigens' residence time in the nasal cavity [9], increasing the chance of uptake by the epithelium. Obviously, a size reduction of the particle from micro to nano scale could be beneficial as nanoparticles (NP) penetrate the nasal epithelium more easily [10, 11]. Once particles have crossed the epithelium they can facilitate the uptake of the antigen by DC. Furthermore, the multimerization of epitopes on the particle surface and the possibility of co-encapsulation with adjuvants can increase the immune recognition by B-cells and other antigen-presenting cells [10, 11].

Evidently, a NP that has all of the above mentioned characteristics is preferred. How such a particle looks like in terms of its physical and chemical properties like material, size, surface charge, physical stability, antigen stability and antigen release profile is currently unknown [12]. In the literature a wide variety of particles, including liposomes, virosomes, oil-in-water emulsions, nanocomplexes and polymer based carriers are mentioned [13], all with a different immunological outcome. For instance, a particle capable of provoking a strong antibody response may fail to trigger the cellular arm of the immune system, or may not induce the production of mucosal, sIgA mediated immunity. This enigma stresses the importance of combining thorough characterization of the delivery system together with *in vitro* analysis of its interaction with immune cells and extensive evaluation of immunological effects *in vivo*.

Two of the most studied polymers for vaccine delivery are undoubtedly poly(lactic-co-glycolic acid) (PLGA) and chitosan (derivatives). Both polymers share the properties to be safe, biodegradable and suitable to prepare (nano)particles. PLGA has been used for controlled

drug release purposes for decades and is therefore an obvious choice for encapsulation of antigen. Because of PLGA's hydrophobic character, PLGA particles are generally prepared by oil-in-water emulsification or solvent evaporation techniques, generally resulting in negatively charged, smooth surfaced and spherical particles. These particles are relatively resistant to salt and pH induced instability, and slowly release their content, based on the hydrolysis rate of the polymer [14]. Promising results for nasal vaccination studies using PLGA particles have been reported [10, 15], but also unsuccessful results have been observed [16], which the authors attributed to the lack of mucoadhesiveness and immune-stimulating factors.

Chitosan (CS) is a (under acidic conditions) water soluble, positively charged polymer and therefore has completely different properties than PLGA. CS particles are often prepared by ionic complexation or spray drying techniques, resulting in positively charged, rather irregular shaped complexes [17, 18]. In contrast to PLGA, CS particles have been described as mucoadhesive and their ability to cross epithelial barriers has been widely accepted. However, they are susceptible to dissociation by exposure to salts and are very unstable at physiological pH [19]. An improvement over CS particles are particles prepared from N-trimethyl chitosan (TMC), a derivate of CS that carries a positive charge independent of the pH. Consequently, TMC particles are much more stable at neutral pH than CS particles. Nasal administration of tetanus toxoid or hemagglutinin loaded TMC nanoparticles (TMC NP) resulted in strong antibody- and hemagglutinin inhibition titers, respectively [20, 21]. Interestingly, recently TMC coated PLGA particles (PLGA/TMC) loaded with Hepatitis B surface antigen have been developed; nasal vaccination of mice with these particles resulted in a marked increase of antigen specific antibodies compared to nasal immunization with HBsAg loaded PLGA particles [22].

This study aims to characterize and compare the physical properties of PLGA NP, TMC NP and TMC-coated PLGA NP (PLGA/TMC NP) loaded with ovalbumin (OVA), a model antigen that elicits little response by itself. The impact of these characteristics on important aspects of nasal vaccination like local toxicity, DC uptake and DC maturation were investigated *in vitro* using a model for ciliary beat frequency (CBF) and human monocyte derived dendritic cells. *In vivo*, nasal residence was investigated using a live fluorescence imaging technique; immunogenicity in terms of systemic and secretory antibody (sub)class titers was investigated after nasal as well as i.m. administration to Balb/c mice. In parallel to these experiments extensive investigation into the T-cell responses resulting from nasal immunization with NP has been performed, the results of which will be presented elsewhere.

Materials and Methods

Materials

Ovalbumin (OVA) was purchased from Calbiochem (Merckbioscience, Beeston,UK). N-trimethyl chitosan with a degree of quaternization of 15% was obtained from 92% deacetylated (MW 120 kDa) chitosan (Primex, Alversham, Norway), by NaOH induced methylation as described by Bal [23]. KCl, NaCl, HNa_2PO_4 and KH_2PO_4 were purchased from Merck (VWR, Amsterdam, The Netherlands). Poly(lactic-co-glycolic acid) (PLGA) 50:50 Mw 5000-15000 Da, pentasodium tripolyphosphate (TPP), 4-(2-hydroxyethyl)-1-piperazine-ethanesulfonic acid (HEPES), Tween 20, dichloromethane (DCM), dimethyl sulfoxide (DMSO), 2-mercapto ethanol and Protease Type XIV were obtained from Sigma-Aldrich (Steinheim, Germany). 10% polyacrylamide SDS-PAGE gels were acquired from Biorad (Veenendaal, The Netherlands). Poly-(ethylenimine) (PEI) was a generous gift from Wim Hennink (Utrecht Institute of Pharmaceutical Sciences, Utrecht, The Netherlands). Goat anti mouse IgG, IgG1, IgG2a or IgA conjugated with horseradish peroxidase was purchased at Southern Biotech (Birmingham, AL). DMEM-Ham's F12 (1:1) medium, Ultroser G and NU-serum were obtained from Life Technologies Ltd. (Paisley, UK). RPMI 1640, Foetal Bovine Serum (FBS), penicillin-streptomycin (P/S) solution, fluorescein isothiocyanate and Alexa fluor 647 conjugated ovalbumin (OVA-FITC and $OVA_{Alexa\ Fluor\ 647}$) and Lysotracker were acquired from Invitrogen (Breda, The Netherlands).

Nanoparticle preparation and characterization

Nanoparticle preparation

TMC NP were prepared by ionic complexation of TMC with TPP. To 5 ml of a 2 mg/ml TMC solution, 1 ml of 0.1 % w/v OVA solution was added under continuous stirring. Subsequently 0.3 ml water, 2 ml 25 mM Hepes pH 7.4 and 1.7 ml 0.1% w/v TPP solution were added. After 15 min of stirring, particles were collected by centrifugation (10000 g, 15 min) on a glycerol bed, washed once with water and finally resuspended in water and stored at 4°C.

PLGA NP were obtained with a double emulsion method. 50 µl of a 1% w/v OVA solution was dispersed in 1 ml 2.5% w/v PLGA in DCM by tip sonication (15 s 20 W). The obtained water-in-oil (w/o) emulsion was dispersed in 2 ml of 1% v/v Tween 20 by sonication (15 s, 20 W). This w/o/w emulsion was added drop wise to a 50 ml warm (40°C) 0.02% v/v Tween 20 aqueous solution (extraction medium) under continuous stirring to extract and evaporate the

DCM. After 1 hour, particles were collected by centrifugation (8000 g, 10 min), washed twice with water to remove free OVA and stored at 4°C until further analysis.

PLGA/TMC NP were prepared as described for the PLGA NP, with the difference that TMC was added to the extraction medium to a final concentration of 80 µg/ml. Using FITC-labelled TMC we estimated that ca. 90% of the added TMC was associated with the PLGA NP. Supernatants were stored at 4°C for determination of the loading efficiency.

NP containing OVA-FITC or $OVA_{Alexa\ Fluor\ 647}$ were prepared in exactly the same manner by replacing OVA with its fluorescent counterpart.

Physical characterization of nanoparticles

Size and morphology of the NP were visualized with scanning electron microscopy (SEM). 50 µl of 0.1% w/v particle suspension was air dried overnight on a metal stub. Particles were gold/palladium sputtered using a sputter coater device K650X (Emitech, Hailsham, UK) and analyzed with a JEOL JSM-6700F scanning electron microscope (Jeol, Tokyo, Japan).

Mean size distribution was determined with dynamic light scattering (DLS) using a NanoSizer ZS (Malvern Instruments, Malvern UK). The zeta potential of the particles was measured by laser Doppler velocimetry using the same apparatus. Before the measurement, samples were diluted in 5 mM Hepes pH 7.4 until a slightly opalescent dispersion was obtained.

Loading efficiency (LE) was calculated from the amount of OVA detected in the supernatant and expressed as percentage of the total amount of OVA added ($LE= 100-(OVA_{sup}/OVA_{tot}*100)$). OVA concentrations were determined with a BCA protein assay (Pierce, Rockford, IL, USA) according to the manufacturer's instructions.

Assessment of antigen release and stability

To determine the release characteristics, NP containing OVA-FITC were diluted to a concentration of 1 mg/ml NP in 5 ml PBS containing 0.01% Tween 20. Dispersions were incubated at 37°C for 25 days under continuous stirring (200 rpm). At different time points, an aliquot (0.30 ml) was taken (and not replaced with fresh PBS). Aliquots were centrifuged for 20 min at 13000 g and supernatants were stored at 4°C until fluorescence intensity was assessed using an FS920 fluorimeter (Edinburgh Instruments, Campus Livingston, UK).

To determine the stability of the antigen, supernatants from OVA loaded particles were collected after 11 days. Residual OVA was extracted from the pellet according to a protocol by Ghassemi *et al* [24]. Briefly, the pellet was freeze dried overnight, and the lyophilized product

was reconstituted in 200 µl DMSO. Subsequently, 800 µl of 0.5 % w/v SDS and 0.05 M NaOH were added and the mixture was left at room temperature for 2 h.

OVA content was determined with BCA protein assay and a total of 0.6 µg OVA was loaded on a 10% poly(acrylamide) gel under reducing conditions. Protein bands were visualized with silver staining (Silver Stain Plus, Biorad) according to the manufacturer's instructions. Western blot analysis was performed as previously reported [25].

Ciliary beat frequency measurements

Cell isolation and culture

Human nasal epithelial cells were isolated from nasal biopsies according to a previously described method [26]. The cells were plated in 12-well plates pre-coated with 0.2% rat tail collagen at a density of $5*10^5$ cells/well in a final volume of 2 ml medium and incubated at 37°C and 5% CO_2. The medium was refreshed 24 h after plating and subsequently every other day. Ciliary beat frequency (CBF) measurements were performed on day eight to ten after plating. All experiments were performed in an air-conditioned room at a constant temperature of 22°C. Cell culture plates were removed from the incubator one hour prior to the experiment, in order to allow the medium to adapt to the environmental temperature. Cells were exposed for 45 minutes to 2.5 ml DMEM-Ham's F12 (1:1) medium (negative control), 0.5 mg/ml or 5 mg/ml of nanoparticle dispersion or 0.5 mg PEI (positive control), after which cells were washed twice with DMEM-Ham's F12 (1:1) medium. Cells were allowed to recover for 90 minutes after which CBF was assessed again.

Data acquisition

An inverted microscope (Olympus IX70) was used at a magnification of 600 times. A MotionScope high-speed digital camera and PCI application software, running in a Windows 2000 environment (Redlake MASD Inc., San Diego, CA), were used for image acquisition. The images were captured at a frame rate of 500 frames per second with a sampling interval of 2 ms, before, after and during exposure to the nanoparticles. A sequence of 1024 images was recorded for each area. Each sequence of frame-by-frame images was stored in a file folder containing 1024 TIF format files for later analysis. CBF was calculated as described before [27, 28].

Dendritic cells studies

Human monocyte derived dendritic cell culture

Monocytes were freshly isolated from human donor blood before each experiment by means of density gradients (Ficoll and Percoll) and depletion of platelets was performed by adherence of the monocytes in 24-well plate (Corning, Schiphol, The Netherlands) followed by washing. Monocytes (5*105 cells/well) were maintained for 6 days in RPMI 1640, supplemented with 10% v/v FBS, 1% v/v glutamine, 1% v/v P/S, GM-CSF 250 U/ml (Biosource-Invitrogen, Breda, The Netherlands,) and IL-4 100 U/ml (Biosource) at 37°C and 5% CO2 to differentiate into immature DC (imDC). Medium was refreshed after 3 days.

Interaction of nanoparticles with dendritic cells

ImDC were incubated for 4 h at 37°C in RPMI 1640 and 500 U/ml GMCSF with 2 µg/ml OVA-FITC either free or encapsulated in TMC, PLGA or PLGA/TMC NP. Cells were washed 3 times with PBS containing 1% w/v bovine serum albumin and 2% v/v FBS before OVA-FITC association with DC was quantified using flow cytometry (FACSCantoII, Becton Dickinson). Live cells were gated based on forward and side scatter. OVA-FITC association was expressed as the mean fluorescence intensity (MFI) in the FL-1 channel.

For confocal microscopy, 50,000 imDC were plated on a poly-lysine coated Petri dish (Corning) and incubated for 30 minutes at 37°C. Cells were washed with PBS, and exposed for 1 h to OVAAlexa Fluor 647 containing formulations. Cells were washed 3 times with PBS and exposed to 1 µM Lysotracker® for 15 minutes. Cells were washed 2 more times before visualization.

Effect of nanoparticles on DC maturation

DC were incubated for 48 h at 37°C in RPMI 1640 and 500 U/ml GMCSF with 2 µg/ml OVA, either free or encapsulated in PLGA, PLGA/TMC or TMC NP and LPS (100 ng/ml) as a positive control. Cells were washed 3 times with PBS containing 1% w/v bovine serum albumin and 2% v/v FBS and incubated for 30 min with a mixture of 50x diluted anti-HLA-DR-FITC, anti-CD83-phycoerythrin(PE) and anti-CD86-allophycocyanin(APC) (Becton Dickinson) on ice, to measure expression of MHCII, CD83 and CD86 molecules on the DC' cell surface, respectively. Cells were washed and expression of MHCII, CD83 and CD86 was quantified using flow cytometry (FACSCantoII, Becton Dickinson), assuming 100% maturation for LPS treated DC. Live cells were gated based on forward and side scatter.

***In vivo* studies**

Determination of nasal residence time

Nasal residence time measurements were performed in accordance to the protocol described by Hagenaars et al. [29]. In short, female Balb/c (nu/nu) mice (Charles River, L'Árbresle, France) mice were lightly anesthetized using isofluorane prior to the administration of 5 µg OVA conjugated to a near infrared dye (IRdye™ 800CW, LI-Cor, USA). Nose was cleaned with a paper towel and immediately fluorescence intensity in the nasal cavity was determined using an IVIS Spectrum® (CaliperLS, USA). Every 10 minutes, fluorescence intensity was determined. Between measurements, mice were conscious.

Administration of antigens, immunization and sampling schedules

Female Balb/c mice received 20 µg OVA per nasal or i.m. administration. One priming dose was followed by 2 nasal or i.m booster doses 3 and 6 weeks after priming. For nasal administration, formulations were applied in a volume of 10 µl PBS, 5 µl per nostril. For i.m. administration, 25 µl of formulation in PBS was injected in the thigh muscle. Blood samples were taken from the tail vein before every immunization and 2 weeks after the final booster dose.

Determination of serum IgG, IgG1, IgG2a and secretory IgA

Microtiter plates were coated with 100 ng OVA in carbonate buffer pH 9.4 for 24 hours at 4°C. To reduce non specific binding, wells were blocked with 1% BSA in PBS for 1 hour at 37°C. Serial dilutions of serum ranging from 20 to $2*10^6$, were applied for 1.5 hours at 37°C, nasal washes were added undiluted. OVA specific antibodies were detected using horseradish peroxidase (HRP) conjugated goat anti mouse IgG, IgG1, IgG2a or IgA (1 hour 37°C) and by incubating with tetramethylbenzidine (TMB)/H_2O_2 in acetate buffer pH 5.5 for 15 min at room temperature. Reaction was stopped with 2 M H_2SO_4 and absorbance was determined at 450 nm with an EL808 microplatereader (Bio-Tek Instruments, Bad Friedrichshall, Germany)

Statistics

All the data of the in vitro studies were analyzed with a one-way ANOVA with Bonneferoni's post-test, with the exception of size and zeta potential measurements, which were analyzed with a Students T-test. Antibody titers were analyzed with a Kruskal-Wallis test with Dunns post-test. Statistics were performed using GraphPad 5.0 for Windows.

Results

Physical characterization of nanoparticles

The NP characteristics are summarized in Table 1. Dynamic light scattering showed fairly monodisperse (PDI<0.25) NP with an average size of about 300 nm (PLGA and TMC NP) or 450 nm (PLGA/TMC NP). PLGA NP carried a negative charge at pH 7.4, whereas TMC NP and PLGA/TMC NP were slightly positively charged. Encapsulation efficiency of OVA (pI 4.8) was much higher in the positively charged particles (71.6% and 60.2%) compared to PLGA NP (34.2% $p<0.05$).

Table 1: Physical properties of OVA-loaded nanoparticles. Values represent mean +/- standard deviation of 5 independently prepared batches.

	Size (nm)	PDI	Zetapotential (mV)	Loading Efficiency (%)
PLGA/OVA	320 +/- 17.9	0.151 +/- 0.033	- 48.2 +/- 0.59	34.2 +/- 3.3
PLGA/TMC/OVA	448 +/- 55.9	0.234 +/- 0.031	24.5 +/- 0.90	71.6 +/- 6.2
TMC15/TPP/OVA	258 +/- 28.8	0.200 +/- 0.020	10.4 +/- 0.20	60.2 +/- 4.1

SEM reveals the size and the shape of the particles after air drying. The mean size of the PLGA and PLGA/TMC NP corresponded well to the size found with DLS. TMC NP appeared to be smaller than measured with the DLS, probably due to dehydration of the sample. PLGA and PLGA/TMC NP had a spherical appearance and a smooth surface (*Figure 1*). In contrast, TMC NP were irregularly shaped and had a ruffled surface area.

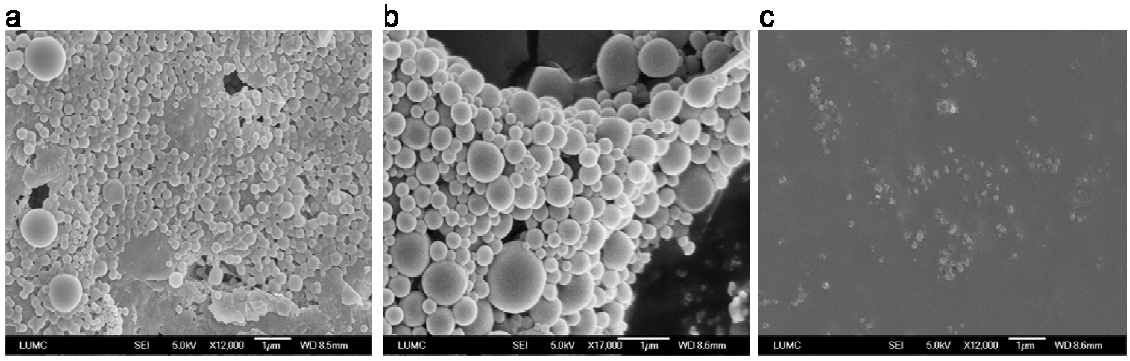

***Figure 1**: Scanning electron microscopy images of OVA-loaded nanoparticles: a) PLGA NP, b) PLGA/TMC NP and c) TMC NP.*

To simulate the stability of the NP after nasal administration, the size of the NP was assessed *in vitro* by incubation in PBS at 37°C (*Figure 2*). PLGA/TMC and TMC NP showed a small (<30%), but not significant ($p>0.05$) size increase, within 8 hours. TMC NP showed signs of aggregation, as the PDI increased ($p<0.05$). No changes in size and PDI values for the PLGA based nanoparticles were observed.

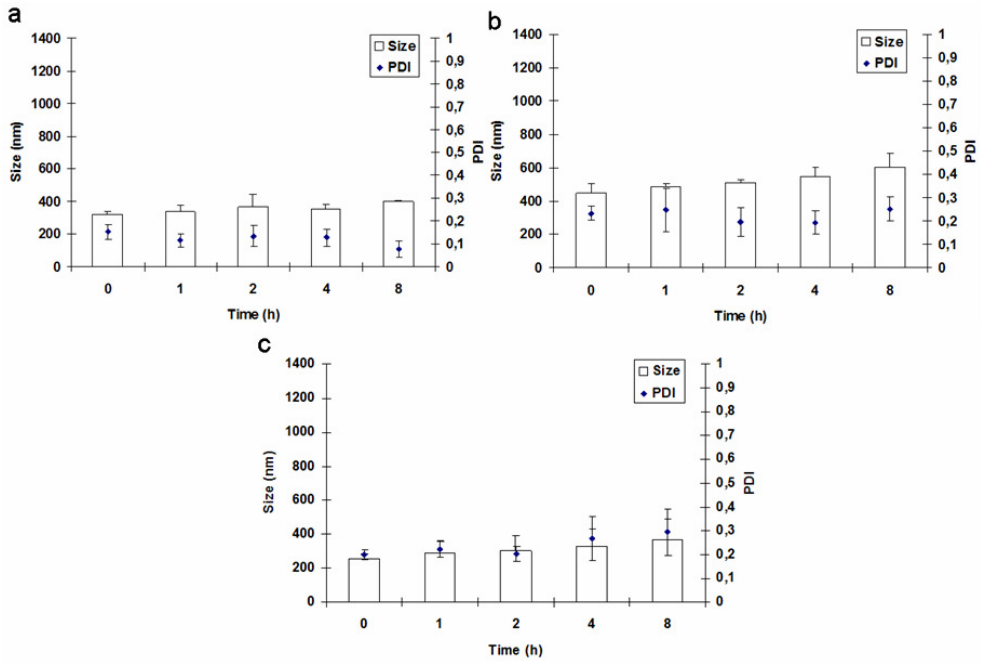

***Figure 2**: Short term (8 h) stability of OVA-loaded NP in PBS at 37°: a) PLGA NP, b) PLGA/TMC NP and c) TMC NP. Results are the average +/- SD of 3 independently prepared batches.*

Antigen release and stability

Release of OVA-FITC from the nanoparticles was monitored over 25 days in PBS pH7.4 at 37°C. PLGA NP showed no significant burst release (*figure 3b*) and up to 80% of their original content in 25 days (*figure 3a*). In contrast, TMC NP showed 20-30% release within the first 24 h, followed by no release over the remainder of 25 days. However, the release of OVA by these particles was enhanced by further dilution in PBS (*figure 3b*), showing that the disintegration of TMC NP is dependent on the concentration and thus is likely to occur very rapidly *in vivo*. This concentration dependent initial release was not observed for PLGA NP. PLGA/TMC NP showed release characteristics of TMC as well as PLGA NP, as a moderate concentration dependent OVA release over the first 24 h was observed (20% at 1 mg/ml, *figure 3b*), followed by progressive release up to 100% after 12 days (*figure 3a*).

As PLGA particles have been described as deleterious for the stability of incorporated biopharmaceuticals [30], the integrity of encapsulated (*Figure 4a*) OVA was investigated with SDS-PAGE and Western blotting. Sonication and contact with DCM did lead to some degradation and aggregation, however the majority of the OVA appeared to be intact with respect to preservation of size and epitopes (*Figure 4a lane 2,4,5*). Moreover, encapsulation in PLGA and TMC NP did not seem to adversely affect the integrity of OVA (*figure 4a lane 4-6*). However, OVA extracted from PLGA and PLGA/TMC was not recognized by anti-OVA IgG antibodies to a similar extent as native OVA or OVA extracted from TMC NP (*figure 4b*), indicating that some of the B-cell epitopes of OVA may have been damaged during the encapsulation process.

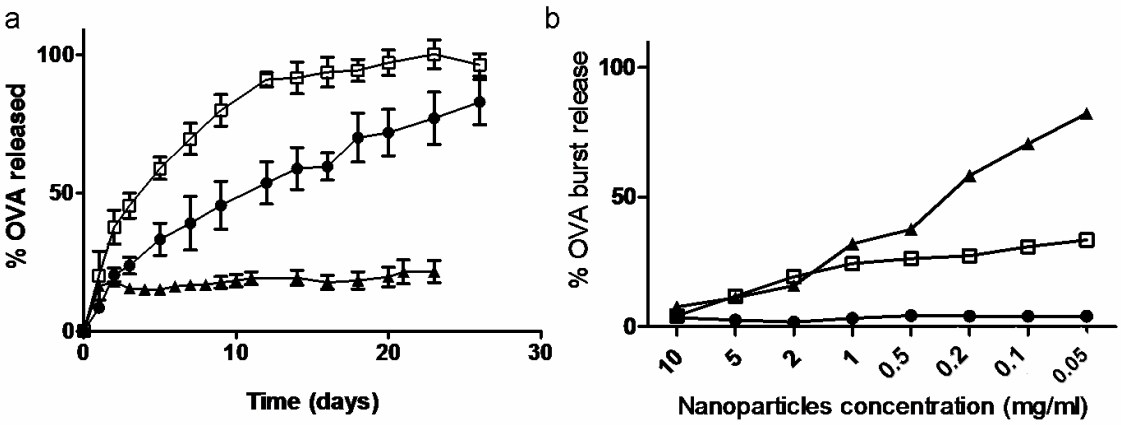

Figure 3: OVA release from PLGA NP (circles), PLGA/TMC NP (squares) and TMC NP (triangles). a) OVA release from 1 mg/ml particle dispersions was monitored over 25 days at 37°C in PBS. b) Burst release of OVA from these particles as function of NP concentration, assessed after 1 h incubation in PBS (pH7.4). Results are the average +/- SD of 3 independently prepared batches.

Toxicity

To explore the safety characteristics of the particles for nasal vaccination, the CBF was measured after 45 min exposure to the particle dispersions in PBS (*Figure 5*). Poly-(ethylenimine) (PEI) was used as positive (toxic) control. Application of a 0.5 mg/ml PEI solution resulted in the complete disappearance of the CBF, within 45 minutes. After removal of the polymer, no recovery of the CBF was recorded. All nanoparticulate formulations were less toxic than PEI solution and did not significantly decrease the CBF. Only at high concentrations (5 mg/ml) TMC/TPP slightly decreased the CBF by about 20% (*data not shown*).

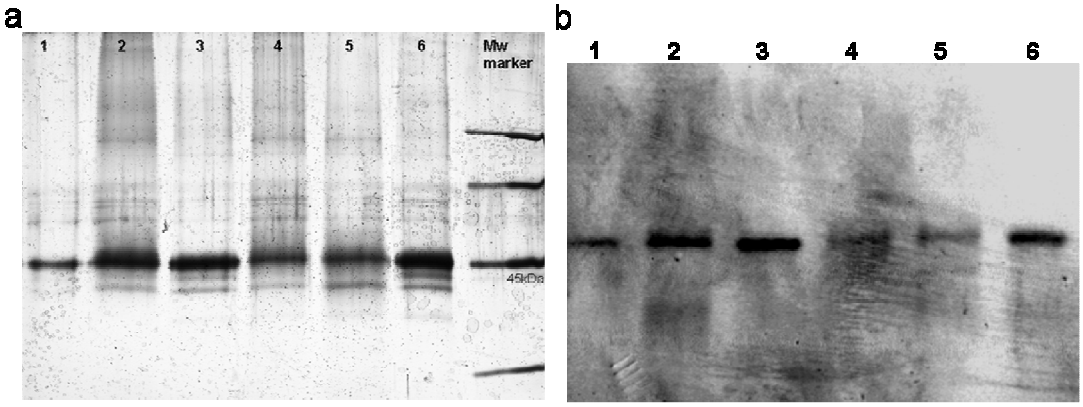

***Figure 4**: Stability of OVA after encapsulation into nanoparticles. a) Silver stained SDS-PAGE gel; b) Anti-OVA Western blot of a second gel run in parallel. 1 = OVA stock solution, 2 = OVA 2x15 s sonicated, 3 = OVA 2x15 s sonicated + DCM extracted, 4 = OVA extracted from PLGA NP, 5 = OVA extracted from PLGA/TMC NP and 6 = OVA extracted from TMC NP. Gel and blot are representative examples of 3 experiments.*

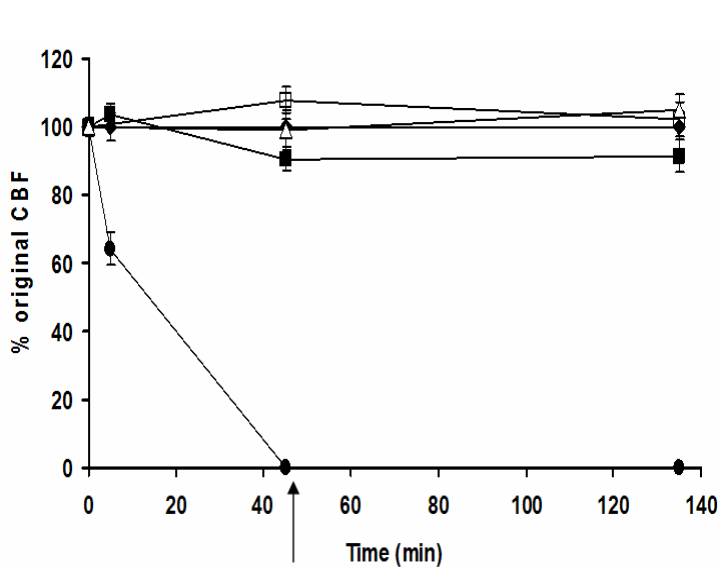

***Figure 5**: Ciliary beat frequency after exposure to 0.5 mg/ml OVA-loaded nanoparticles as a measure for nasal cilia toxicity. Nasal epithelium was exposed for 45 min to formulations, after which the epithelium was washed (arrow) and the CBF allowed to recover for 90 min. Closed diamond = non-exposed, closed circle= PEI solution (0.5 mg/ml), open square= PLGA, open triangle= PLGA/TMC and closed square= TMC/TPP. Data represent mean of 3 donors +/- SD.*

Nasal residence time

Prolonging the residence time of an antigen may be crucial for nasal delivery, as it increases the chance of absorption into the nasal epithelium. Using a fluorescent label we were able to study the clearance of OVA from the nasal cavity. An exponential decay in fluorescence intensity was observed for all formulations (*Figure 6*). The data could be reasonably fitted by an exponential decay function, from which apparent first-order clearance rate constants were determined (*Figure 6 insert*). Compared to an OVA solution, only TMC NP significantly decreased the clearance rate ($p<0.01$). The particulate structure of PLGA NP did not have an effect on the clearance rate of OVA, nor did a TMC coating around it.

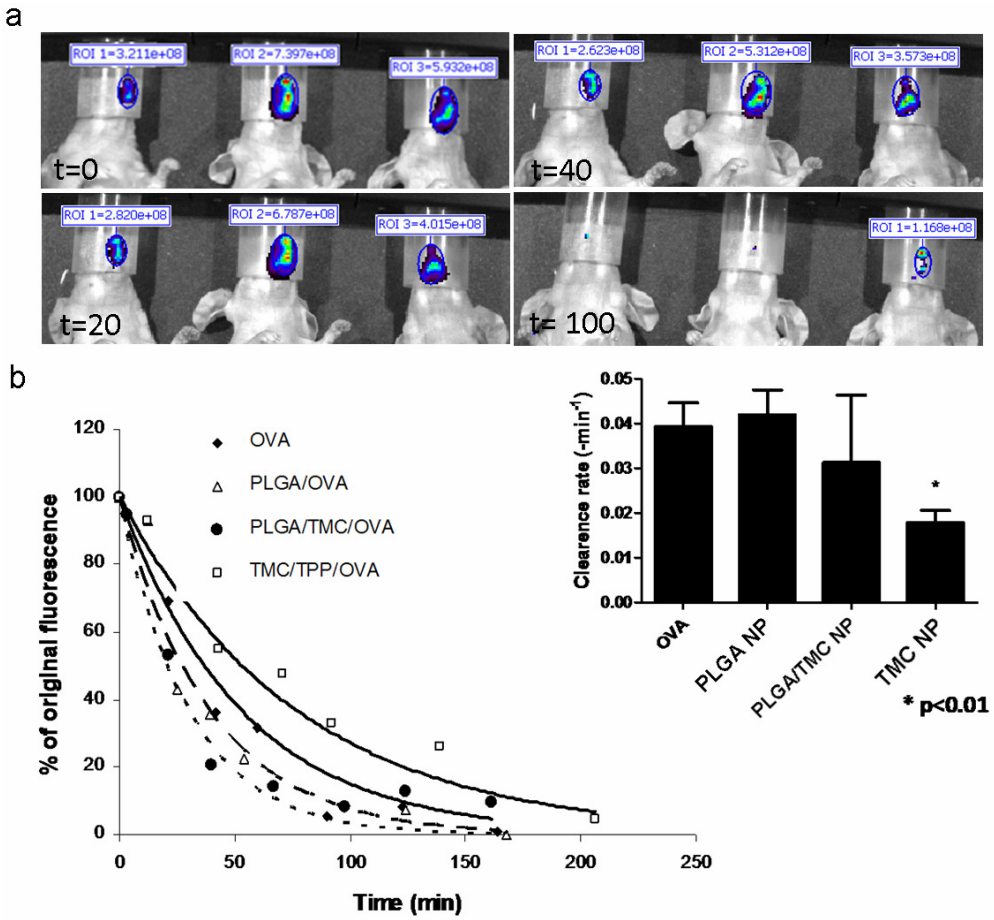

***Figure 6**: Nasal residence time of OVA determined using fluorescence detection of OVA-IRdye CW 800. a) Emission (λ=800 nm) 0, 20, 40 and 100 min after nasal administration of OVA-IRdye CW 800. b) Intensity of fluorescence signal from the nasal cavity normalized for time point 0. Individual time points were fitted using a model for exponential decay. b-insert) apparent first-order clearance rate constants of OVA from the nasal cavity were derived from exponential fits. Data represent mean +/- SD of n=3. * p<0.01*

Dendritic cells studies

Interaction and uptake of the nanoparticles by monocyte derived DC was studied using flow cytometry (*Figure 7a*) and confocal microscopy (F*igure 7b,c*). The positively charged particles (PLGA/TMC NP and TMC NP) interacted strongly with DC compared to PLGA NP and OVA alone ($p<0.05$). However, in the same experiment conducted at 4°C similar fluorescence levels for PLGA/TMC NP and TMC NP treated cells were observed, indicating that the fluorescence was mainly caused by association to the cell membrane rather than uptake by the DC. Indeed, confocal microscopy showed little evidence for TMC NP uptake (nor PLGA/TMC uptake, data not shown) by DC as the particles were almost exclusively detected on the outside of the cell membrane (*Figure 7c*). This is in contrast to a solution of OVA which accumulated in lysosomal compartments (*Figure 7b*).

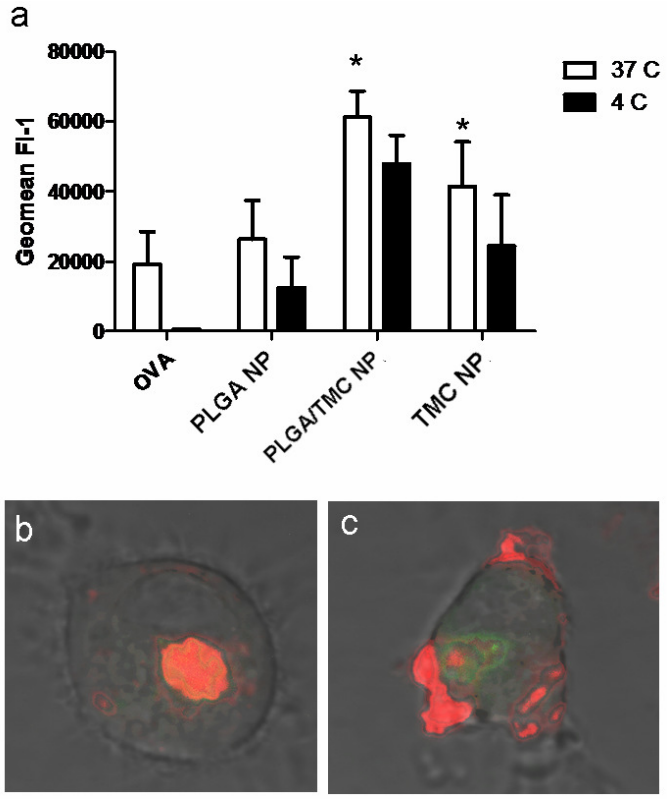

***Figure 7**: Interaction of OVA-loaded nanoparticles with DC. a) Association of particles with human DC quantified using flow cytometric analysis. Bars represent mean +/- SD of 6 different monocytes donors. *p<0.05 compared to OVA 37°C. Merged confocal microscopy image of DC exposed to b) $OVA_{alexafluor647}$ (Red) and Lysotracker® (Green) or c) $TMC/TPP/OVA_{alexafluor647}$ and Lysotracker. Orange corresponds to OVA colocalizing with lysosomes.*

Despite being poorly taken up by DC, TMC NP were able to induce DC maturation (*figure 8*). Although the expression of all measured maturation markers was not as extensive as after LPS exposure, it was significantly increased ($p<0.05$) compared to OVA or PLGA NP, both of

which did not result in increased DC maturation. Again TMC coated PLGA NP appeared to be the middle ground between PLGA and TMC NP, as all maturation markers seemed to be a bit upregulated, but only MHCII to a significant extent.

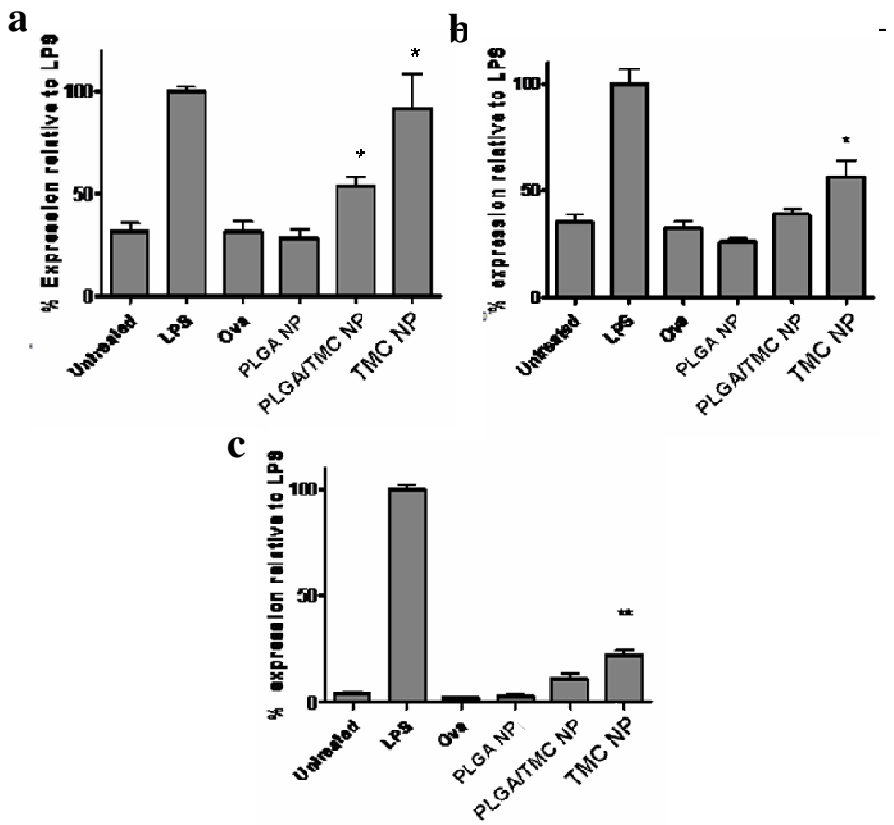

***Figure 8**: DC maturation after 48h stimulation with OVA-containing nanoparticles. Levels of a) MHCII, b) CD83 and c) CD86 were expressed as a percentage of LPS stimulated DC. Histogram represents the mean of 6 independent experiments. Error bars are SEM. * p<0.05 **p<0.01 vs. OVA-treated DC.*

Immunogenicity

Nasal vaccination revealed considerable differences between the NP. Negligible IgG titers were detected after nasal vaccination with PLGA NP and PLGA/TMC NP, whereas only a priming dose of TMC NP was necessary ($p<0.001$ compared to OVA) to induce detectable OVA specific IgG antibodies (*figure 9*). After the 3 nasal challenges, TMC NP immunized mice even

showed similar IgG titers as their i.m. vaccinated counterparts. Furthermore, only nasal washes from TMC NP nasally immunized mice contained OVA specific sIgA (*figure 10b*). All mice responded to i.m. immunization, irrespective of the formulation administered (*figure 9*). However, the NP formulations were more immunogenic than an OVA solution. Both PLGA NP and TMC NP elicited high IgG titers after a priming dose, whereas the titers induced by PLGA/TMC NP were only slightly higher than the OVA induced titers ($p<0.01$). Vaccination with PLGA NP caused a significant shift in the IgG1/IgG2a ratio towards IgG2a compared to i.m. OVA vaccination (*figure 10a*).

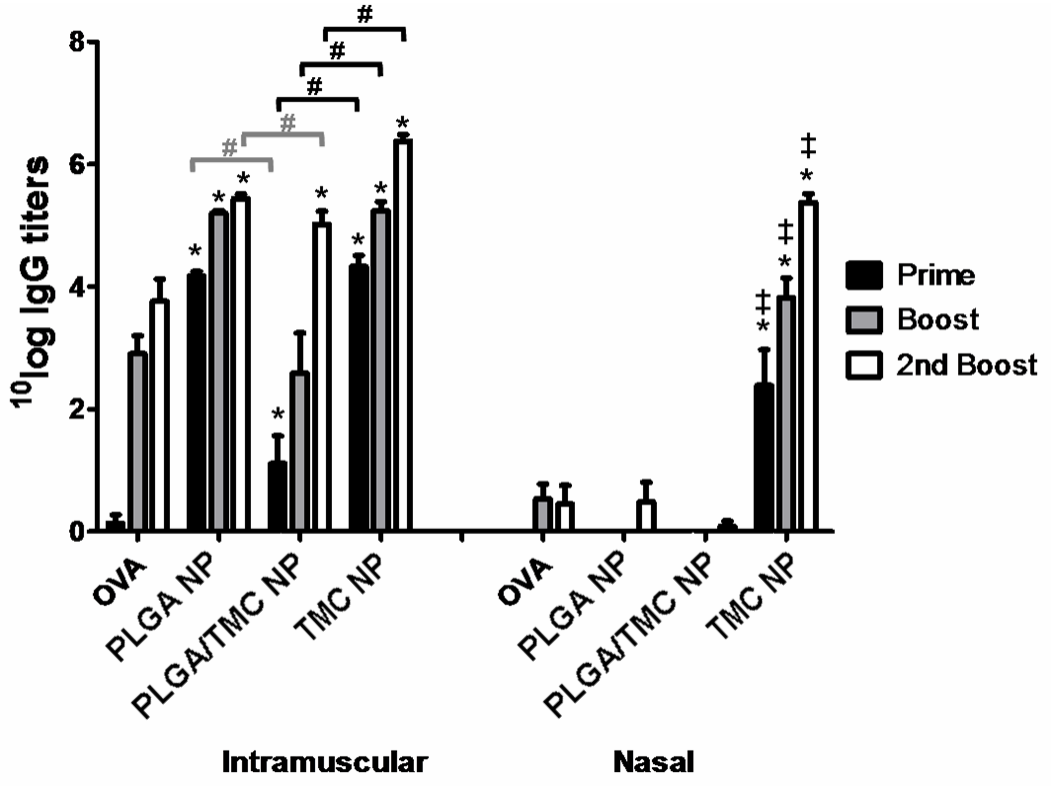

***Figure 9**: OVA specific IgG titers in serum of Balb/c mice 3 weeks after a priming, booster and 2nd booster dose of 20 µg OVA administered i.m. or nasally. Data represent mean +/- SEM, n=8. * p<0.05 compared to OVA i.m., ‡ p<0.05 compared to OVA nasal, # p<0.05.*

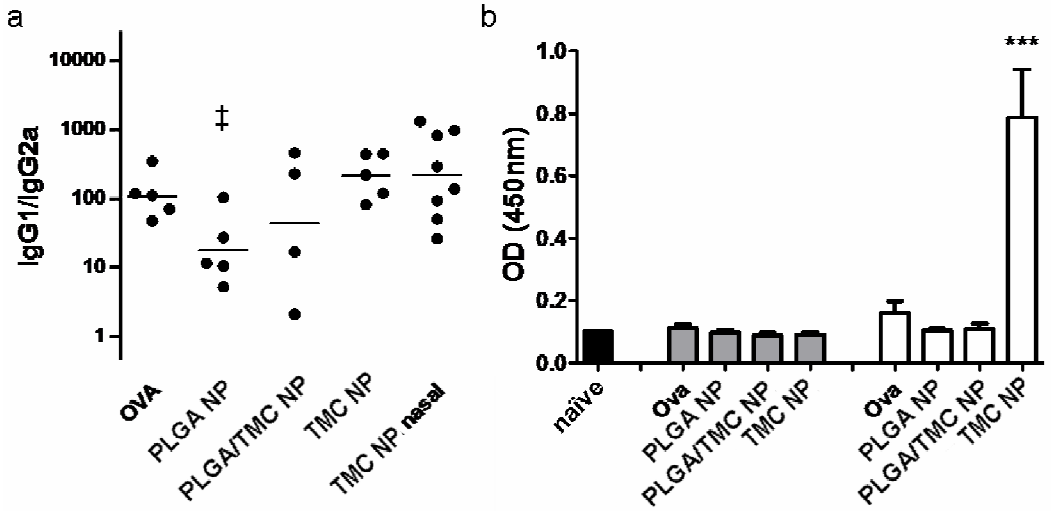

Figure 10**: a) IgG1/IgG2a balance after i.m. vaccination, and for TMC NP also after nasal vaccination. ‡ p<0.05 compared to OVA. Bar represents mean. b) OVA specific sIgA in nasal washes of mice after i.m. (grey bars) or nasal (white bars) administration. Bars represent mean (i.m. n=5, nasal n=8) +/- SEM . p<0.001 compared to naïve mice.*

Discussion

Although nanoparticles have been described as very promising nasal vaccine carriers [8, 13], surprisingly little is known about the physicochemical properties of nanoparticles in relation to the immune response they elicit. The particle size is probably one of the parameters which is most adequately described, as several studies using micro- and nanoparticles point to smaller particles being more immunogenic [8, 10, 11, 31-33]. Studies by Jung et al. and Gutierro et al. seem to indicate, however, that intranasally applied antigen-loaded particles of about 200 nm and 500 nm do not differ in immunogenicity [10, 32]. As the nanoparticles in our present study were all smaller than 500 nm and showed only minor differences in size compared to the above range, size variation between the particles is most probably not the factor that caused the differences in immunogenicity. To a somewhat lesser extent, the zeta potential of particles has been investigated, leading to the conclusion that a positive surface charge may be favourable in nasal vaccination [9, 21, 34, 35]. The result of our present study supports that conclusion, as the positively charged TMC NP outperformed the negatively charged PLGA NP after nasal administration. However, it is also clear that the zeta potential is not the sole determinant of the resulting antibody responses. TMC and PLGA/TMC

NP are both positively charged, but TMC NP induced superior IgG titers compared to PLGA/TMC NP.

Although measuring immune responses after nasal administration of antigen loaded nanoparticles is very useful, it restricts us to a mere trial-and-error based approach of nasal vaccine design. For instance, it does not answer the question why PLGA/TMC NP elicit a different immune response than TMC NP. Both particles are in the same size range and do not contain any known immunomodulatory substances other than TMC [20, 36, 37]. Focusing on the various aspects of nasal vaccination; like the clearance from the nasal cavity, the uptake by DC and the maturation of antigen-presenting cells as function of particle characteristics may answer this question and would allow us to improve nanoparticulate vaccine carriers in a rational way. Using this approach, we were able to explain differences in immunogenicity between PLGA, PLGA/TMC and TMC NP. Both PLGA and PLGA/TMC NP failed to elicit an antibody response after nasal vaccination. Nonetheless, after i.m. administration both particles induced higher IgG titers than OVA, implying that these particles can augment the immune response, but are not suitable for nasal administration. In contrast, TMC NP elicited strong antibody responses via both vaccination routes, indicating that TMC NP have certain characteristics which are profitable for nasal vaccination.

Like PLGA and PLGA/TMC NP, TMC NP were found not to be toxic to the cilia (*figure 5*) or mucosal epithelial cells [38-40] and are therefore likely do not damage the nasal epithelium. TMC NP do not promote the uptake by DC (*figure 7*), but do prolong the residence time of OVA in the nasal cavity (*figure 6*), compared to PLGA and PLGA/TMC NP. The nasal residence time of OVA encapsulated in the particles correlates with the IgG titers of mice nasally challenged with these particles, suggesting that the difference in immunogenicity between the particles is related to the delivery of antigen into the nasal epithelium.

PLGA's immunopotentiating effect after parenteral administration has been attributed to its slow release characteristics, leading to a depot formation and subsequently causing enhanced B-cell and T-cell proliferation [41-43]. Indeed, PLGA and PLGA/TMC NP released their content over a prolonged period of time (*figure 3*) and showed an increased antibody response when administered by i.m. injection. PLGA/TMC NP released OVA faster than PLGA *in vitro*, which may contribute to the slightly lower IgG titers in mice immunized i.m. with PLGA/TMC NP, as compared to the PLGA NP group. Although depot formation can be a mechanism to potentiate the immune response after parenteral injections, it is very unlikely that it is a driving force behind nasal vaccination, as the nasal residence time is limited. Moreover, in contrast to uptake by DC, antigen uptake by B-cells is a highly specific process mediated by the contact of the antigen with the B-cell receptor [44]. Therefore, uptake of OVA

by B-cells will be dependent on either surface coated or released OVA and encapsulated antigen is not easily taken up by B-cells [45]. As a consequence, for nasal vaccination a slow release rate may be detrimental as only little time for B-cell uptake is available. Keijzer *et al*. indeed showed that nasal immunization of mice with TMC NP and to a lesser extent PLGA/TMC, but not PLGA NP, results in OVA specific B-cells in the nasal associated lymphoid tissue and in cervical lymph nodes (manuscript in preparation). In the same study nasal immunization with PLGA NP or PLGA/TMC NP of mice which received an adoptive transfer of OVA specific $CD4^+$ T-cells showed effective T-cell activation and proliferation in the nasal associated lymphoid tissue and cervical lymph nodes. This indicates that PLGA and PLGA/TMC NP do cross the nasal epithelium and are taken up by DC (which in turn are capable of activating T-cells), but do not deliver their antigen to B-cells as effectively as TMC NP.

Finally, the nasal epithelium is renowned for being a tolerogenic site, making maturation of imDC into mature DC essential for an effective nasal vaccine. TMC NP were shown to stimulate the maturation of imDC, which may contribute to TMC NP's effectiveness as a nasal adjuvant. OVA-loaded PLGA particles have been reported before not to increase DC maturation [39, 46] and although TMC has been reported as an adjuvant [23], the addition of TMC to the PLGA particles only caused a small increase in expression of maturation markers (Figure 8). This could be explained by the substantially higher ratio TMC:OVA in the TMC NP compared to the PLGA/TMC particles (10:1 vs. 2:1), or to the different architecture of TMC NP versus PLGA/TMC particles.

The data presented in this study indicate that contributing factors to TMC NP being a good nasal vaccine carrier system may be that they (i) prolong the nasal residence time of its incorporated antigen, (ii) quickly release the antigen to promote the formation of OVA specific B-cells and (iii) effectively induce DC maturation breaking the nasal tolerance. However, TMC NP vaccinated mice showed little evidence of activation of the cellular arm of the immune system; the IgG1 titers far exceeded the IgG2a titers (*figure 10a*). This is in line with previous studies demonstrating that the use of TMC as an adjuvant induces Th2 type responses [20, 23, 47]. The addition of a Th1 skewing adjuvant (like CpG) to the TMC NP could make these carriers a more complete nasal vaccine formulation.

Conclusion

The composition and characteristics of nanoparticles greatly influence the extent and the type of immune response elicited after nasal vaccination. TMC NP were shown to be superior over PLGA NP and PLGA/TMC NP in the elicitation of antibody responses after nasal administration. This may be due to their mucoadhesiveness, the rapid release of the contained antigen, and immune stimulatory capacity, in order to respectively prolong the nasal residence time, promote uptake by B-cells and activate DCs.

Acknowledgements

This research was performed under the framework of TI Pharma project number D5-106 “vaccine delivery: alternatives for conventional multiple injection vaccines”.

References

1. Debin, A., et al., *Intranasal immunization with recombinant antigens associated with new cationic particles induces strong mucosal as well as systemic antibody and CTL responses.* Vaccine, 2002. **20**(21-22): p. 2752-63.
2. Hamdy, S., et al., *Enhanced antigen-specific primary CD4+ and CD8+ responses by codelivery of ovalbumin and toll-like receptor ligand monophosphoryl lipid A in poly(D,L-lactic-co-glycolic acid) nanoparticles.* J Biomed Mater Res A, 2007. **81**(3): p. 652-62.
3. Khatri, K., et al., *Plasmid DNA loaded chitosan nanoparticles for nasal mucosal immunization against hepatitis B.* Int J Pharm, 2008. **354**(1-2): p. 235-41.
4. Read, R.C., et al., *Effective nasal influenza vaccine delivery using chitosan.* Vaccine, 2005. **23**(35): p. 4367-74.
5. Revaz, V., et al., *Humoral and cellular immune responses to airway immunization of mice with human papillomavirus type 16 virus-like particles and mucosal adjuvants.* Antiviral Res, 2007. **76**(1): p. 75-85.
6. Sloat, B.R. and Z. Cui, *Strong mucosal and systemic immunities induced by nasal immunization with anthrax protective antigen protein incorporated in liposome-protamine-DNA particles.* Pharm Res, 2006. **23**(2): p. 262-9.
7. Sorichter, S., et al., *Immune responses in the airways by nasal vaccination with systemic boosting against Pseudomonas aeruginosa in chronic lung disease.* Vaccine, 2009. **27**(21): p. 2755-9.
8. Koping-Hoggard, M., A. Sanchez, and M.J. Alonso, *Nanoparticles as carriers for nasal vaccine delivery.* Expert Rev Vaccines, 2005. **4**(2): p. 185-96.
9. Jaganathan, K.S. and S.P. Vyas, *Strong systemic and mucosal immune responses to surface-modified PLGA microspheres containing recombinant hepatitis B antigen administered intranasally.* Vaccine, 2006. **24**(19): p. 4201-11.
10. Gutierro, I., et al., *Size dependent immune response after subcutaneous, oral and intranasal administration of BSA loaded nanospheres.* Vaccine, 2002. **21**(1-2): p. 67-77.
11. Vila, A., et al., *PLA-PEG particles as nasal protein carriers: the influence of the particle size.* Int J Pharm, 2005. **292**(1-2): p. 43-52.
12. Sharma, S., et al., *Pharmaceutical aspects of intranasal delivery of vaccines using particulate systems.* J Pharm Sci, 2009. **98**(3): p. 812-43.
13. Slütter, B., N. Hagenaars, and W. Jiskoot, *Rational design of nasal vaccines.* J Drug Target, 2008. **16**(1): p. 1-17.
14. Corrigan, O.I. and X. Li, *Quantifying drug release from PLGA nanoparticulates.* Eur J Pharm Sci, 2009. **37**(3-4): p. 477-85.
15. Gutierro, I., et al., *Influence of dose and immunization route on the serum Ig G antibody response to BSA loaded PLGA microspheres.* Vaccine, 2002. **20**(17-18): p. 2181-90.
16. Lemoine, D., et al., *Intranasal immunization against influenza virus using polymeric particles.* J Biomater Sci Polym Ed, 1999. **10**(8): p. 805-25.
17. Boddohi, S., et al., *Polysaccharide-Based Polyelectrolyte Complex Nanoparticles from Chitosan, Heparin, and Hyaluronan.* Biomacromolecules, 2009. **77**(1): p. 60-8.
18. Gan, Q., et al., *Modulation of surface charge, particle size and morphological properties of chitosan-TPP nanoparticles intended for gene delivery.* Colloids Surf B Biointerfaces, 2005. **44**(2-3): p. 65-73.
19. Amidi, M., et al., *Chitosan-based delivery systems for protein therapeutics and antigens.* Adv Drug Deliv Rev, 2010. **62**(1): p. 59-82.
20. Amidi, M., et al., *N-trimethyl chitosan (TMC) nanoparticles loaded with influenza subunit antigen for intranasal vaccination: biological properties and immunogenicity in a mouse model.* Vaccine, 2007. **25**(1): p. 144-53.

21. Sayin, B., et al., *Mono-N-carboxymethyl chitosan (MCC) and N-trimethyl chitosan (TMC) nanoparticles for non-invasive vaccine delivery.* Int J Pharm, 2008. **363**(1-2): p. 139-48.
22. Pawar, D., et al., *Evaluation of Mucoadhesive PLGA Microparticles for Nasal Immunization.* AAPS J, 2010. **12**(2): p. 130-7.
23. Bal, S.M., et al., *Efficient induction of immune responses through intradermal vaccination with N-trimethyl chitosan containing antigen formulations.* J Control Release, 2009. **142**(3): p. 374-83.
24. Ghassemi, A.H., et al., *Preparation and characterization of protein loaded microspheres based on a hydroxylated aliphatic polyester, poly(lactic-co-hydroxymethyl glycolic acid).* J Control Release, 2009. **138**(1): p. 57-63.
25. Slütter, B., et al., *Conjugation of ovalbumin to trimethyl chitosan improves immunogenicity of the antigen.* J Control Release, 2010. **143**(2): p. 207-14.
26. Jorissen, M., et al., *Ciliogenesis and coordinated ciliary beating in human nasal epithelial cells cultured in vitro.* Acta Otorhinolaryngol Belg, 1989. **43**(1): p. 67-73.
27. Mallants, R., M. Jorissen, and P. Augustijns, *Effect of preservatives on ciliary beat frequency in human nasal epithelial cell culture: single versus multiple exposure.* Int J Pharm, 2007. **338**(1-2): p. 64-9.
28. Dimova, S., et al., *High-speed digital imaging method for ciliary beat frequency measurement.* J Pharm Pharmacol, 2005. **57**(4): p. 521-6.
29. Hagenaars, N., et al., *Role of trimethylated chitosan (TMC) in nasal residence time, local distribution and toxicity of an intranasal influenza vaccine.* J Control Release, 2010. **144**(1): p. 17-24.
30. van de Weert, M., *Structural integrity of pharmaceutical proteins in polymeric matrices*, in *Biopharmacy and Pharmaceutical Technology*. 2001, Utrecht University: Utrecht. p. 168.
31. Fujimura, Y., et al., *Uptake of microparticles into the epithelium of human nasopharyngeal lymphoid tissue.* Med Mol Morphol, 2006. **39**(4): p. 181-6.
32. Jung, T., et al., *Tetanus toxoid loaded nanoparticles from sulfobutylated poly(vinyl alcohol)-graft-poly(lactide-co-glycolide): evaluation of antibody response after oral and nasal application in mice.* Pharm Res, 2001. **18**(3): p. 352-60.
33. Sandri, G., et al., *Nanoparticles based on N-trimethylchitosan: evaluation of absorption properties using in vitro (Caco-2 cells) and ex vivo (excised rat jejunum) models.* Eur J Pharm Biopharm, 2007. **65**(1): p. 68-77.
34. Baca-Estrada, M.E., M. Foldvari, and M. Snider, *Induction of mucosal immune responses by administration of liposome-antigen formulations and interleukin-12.* J Interferon Cytokine Res, 1999. **19**(5): p. 455-62.
35. Joseph, A., et al., *A new intranasal influenza vaccine based on a novel polycationic lipid--ceramide carbamoyl-spermine (CCS) I. Immunogenicity and efficacy studies in mice.* Vaccine, 2006. **24**(18): p. 3990-4006.
36. Hagenaars, N., et al., *Physicochemical and immunological characterization of N,N,N-trimethyl chitosan-coated whole inactivated influenza virus vaccine for intranasal administration.* Pharm Res, 2009. **26**(6): p. 1353-64.
37. Slütter, B., et al., *Mechanistic study of the adjuvant effect of biodegradable nanoparticles in mucosal vaccination.* J Control Release, 2009.
38. Amidi, M., et al., *Preparation and characterization of protein-loaded N-trimethyl chitosan nanoparticles as nasal delivery system.* J Control Release, 2006. **111**(1-2): p. 107-16.
39. Slütter, B., et al., *Mechanistic study of the adjuvant effect of biodegradable nanoparticles in mucosal vaccination.* J Control Release, 2009. **138**(2): p. 113-21.
40. Verheul, R.J., et al., *Synthesis, characterization and in vitro biological properties of O-methyl free N,N,N-trimethylated chitosan.* Biomaterials, 2008. **29**(27): p. 3642-9.
41. Luzardo-Alvarez, A., et al., *Biodegradable microspheres alone do not stimulate murine macrophages in vitro, but prolong antigen presentation by macrophages in vitro and stimulate a solid immune response in mice.* J Control Release, 2005. **109**(1-3): p. 62-76.
42. Kanchan, V., Y.K. Katare, and A.K. Panda, *Memory antibody response from antigen loaded polymer particles and the effect of antigen release kinetics.* Biomaterials, 2009. **30**(27): p. 4763-76.

43. Waeckerle-Men, Y. and M. Groettrup, *PLGA microspheres for improved antigen delivery to dendritic cells as cellular vaccines.* Adv Drug Deliv Rev, 2005. **57**(3): p. 475-82.
44. Trombetta, E.S. and I. Mellman, *Cell biology of antigen processing in vitro and in vivo.* Annu Rev Immunol, 2005. **23**: p. 975-1028.
45. Dal Monte, P. and F.C. Szoka, Jr., *Effect of liposome encapsulation on antigen presentation in vitro. Comparison of presentation by peritoneal macrophages and B cell tumors.* J Immunol, 1989. **142**(5): p. 1437-43.
46. Fischer, S., et al., *The preservation of phenotype and functionality of dendritic cells upon phagocytosis of polyelectrolyte-coated PLGA microparticles.* Biomaterials, 2007. **28**(6): p. 994-1004.
47. Hagenaars, N., et al., *Relationship between structure and adjuvanticity of N,N,N-trimethyl chitosan (TMC) structural variants in a nasal influenza vaccine.* J Control Release, 2009. **140**(2): p. 126-33.